Available online at www.sciencedirect.com
SCIENCE DIRECT®
Bioorganic & Medicinal Chemistry 13 (2005) 6394–6403
Bioorganic & Medicinal Chemistry

Structure–activity studies of uptake and phototoxicity with heavy-chalcogen analogues of tetramethylrosamine in vitro in chemosensitive and multidrug-resistant cells

Scott L. Gibson,[a] Jason J. Holt,[b] Mao Ye,[b] David J. Donnelly,[b] Tymish Y. Ohulchanskyy,[c] Youngjae You[b] and Michael R. Detty[b,c,*]

[a]*Department of Biochemistry and Biophysics, University of Rochester Medical Center, 601 Elmwood Avenue, PO Box 712, Rochester, NY 14641, USA*
[b]*Department of Chemistry, University at Buffalo, The State University of New York, Buffalo, NY 14260, USA*
[c]*Institute for Lasers, Photonics, and Biophotonics, University at Buffalo, The State University of New York, Buffalo, NY 14260, USA*

Received 22 May 2005; revised 26 June 2005; accepted 27 June 2005
Available online 9 August 2005

Abstract—Several thio and seleno analogues of tetramethylrosamine (**TMR**) were prepared. Thio derivatives of **TMR** have absorption maxima near 570 nm, while seleno derivatives of **TMR** have absorption maxima near 580 nm. The 3- or 4-*N*,*N*-dimethylaminophenyl substituent in the 9-position greatly increases internal conversion, which lowers quantum yields for fluorescence and the generation of singlet oxygen. Thio and seleno analogues of **TMR** are effective photosensitizers against chemosensitive AUXB1 cells in vitro and against multidrug-resistant CR1R12 cells in vitro, which have been treated with verapamil. The CR1R12 cells accumulated significantly lower concentrations of the photosensitizers relative to the AUXB1 cells presumably due to the expression of P-glycoprotein (Pgp) in the CR1R12 cells. Following treatment with 5×10^{-5} M verapamil, the uptake in CR1R12 cells of several fluorescent thio analogues of **TMR** is comparable to that observed for the chemosensitive AUXB1 cells.

1. Introduction

Multidrug resistance (MDR) has been identified as a major impediment to successful chemotherapy for a variety of cancers.[1] Multidrug resistance is attributed to the action of a class of membrane proteins termed the ATP-binding cassette (ABC) transporters.[1–3] These proteins, P-glycoprotein (Pgp), the multidrug resistance protein (MRP) series, breast cancer resistance protein (BCRP), and lung-resistance-related protein (LRP), are involved in the transport of substrates that span a wide range of chemically diverse and structurally disparate compounds including a majority of the commonly prescribed chemotherapeutic agents.[4] The ABC transport proteins possess similarities such as their dependence on the energy derived from ATP hydrolysis to transport substrates,[5] the presence of units of six transmembrane domains (TMDs) which are poorly conserved among the different proteins, and the presence of nucleotide-binding domains (NBDs) which are highly conserved.[1–3] The majority of the ABC transporters are responsible for the transmembrane movement of ions and compounds to maintain levels necessary for cell viability. The drug resistance proteins in this class, of which P-glycoprotein is reportedly the most prevalent,[6] have the unique ability to pump a broad array of chemotherapeutics actively out of the cells, dramatically reducing drug concentration and thus their therapeutic effectiveness.[1,6] Interestingly, expression of Pgp and its recognition of various substrates can be induced by exposure to a single compound or therapeutic agent.[7] Due to the diverse nature of the molecules transported by Pgp, its function as an efflux pump is of major concern for clinicians and under intense investigation by numerous groups worldwide.[8]

Attempts have been made to alleviate the function of Pgp using modulators such as verapamil, quinidine,

Keywords: Tetramethylrosamine; Thiotetramethylrosamine; Selenotetramethylrosamine; Photodynamic therapy; Multidrug resistance.
* Corresponding author. Tel.: +1 716 645 6800x2200; fax: +1 716 645 6963; e-mail: mdetty@buffalo.edu

0968-0896/$ - see front matter © 2005 Elsevier Ltd. All rights reserved.
doi:10.1016/j.bmc.2005.06.056

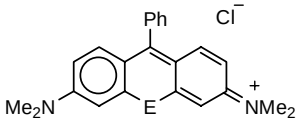

TMR, E = O
TMR-S, E = S
TMR-Se, E = Se

Chart 1. Structure of tetramethylrosamine (**TMR**) and thio- (**TMR-S**) and seleno-analogues (**TMR-Se**).

cyclosporin A, PSC833, and others.[1,9] These modulators bind to the drug-transport-binding site(s) on the protein and impede the binding and subsequent efflux of agent(s) of interest, thus allowing their accumulation.

Studies of the efflux function of Pgp have traditionally used Pgp transport molecules that are either intrinsically fluorescent or tagged with a fluorescent marker.[10,11] Assays employing such compounds usually monitor the efflux of a specific molecule, such as Rhodamine 123, from cells by measuring a decrease in intracellular fluorescence.[11] In addition, the quenching of tetramethylrosamine (**TMR**) fluorescence has been used to measure transport by Pgp in isolated membrane vesicles.[12]

We have been studying heavy-chalcogen analogues of the rhodamine dyes and **TMR** (Chart 1) for their utility as phototoxic agents for malignant cells and tissues.[13,14] These compounds have an affinity for mitochondrial localization in cancer cells due to their delocalized positive charge. The insertion of the heavy-chalcogen atoms sulfur, selenium, or tellurium into these compounds, replacing oxygen in the rhodamines and **TMR**, allows for higher triplet yields and, consequently, higher quantum yields for the generation of singlet oxygen ($^1O_2$). The generation of $^1O_2$ results in damage to intracellular structures and functions ultimately leading to cell death. The use of photosensitizers in combination with Pgp modulators can reduce toxicity toward normal tissues during treatment of multidrug-resistant cancers since the activating light for the photosensitizer can be delivered specifically to the areas of treatment. We extend our initial studies of thiotetramethylrosamine (**TMR-S**) and selenotetramethylrosamine (**TMR-Se**) as photosensitizers for both chemosensitive and multidrug-resistant cells, as transport molecules for Pgp, and as inhibitors of Pgp-mediated multidrug resistance[15] to include a series of structurally related derivatives. In this report, we compare the uptake and phototoxicity of a series of thio and selenotetramethylrosamine analogues in chemosensitive AUXB1 cells and in multidrug-resistant, highly Pgp-expressing CR1R12 cells in which Pgp function has been inhibited by the addition of verapamil. In the presence of verapamil, several of the thiotetramethylrosamine derivatives are effective photosensitizers for multidrug-resistant CR1R12 cells.

2. Results

2.1. Synthesis and properties of dyes 3–12

The synthetic approach to the synthesis of **TMR-S** and **TMR-Se** involves the addition of phenylmagnesium bromide to chalcogenoxanthen-9-ones **1** and **2**, respectively, followed by acid-induced dehydration and ion exchange.[14] To investigate structure–activity relationships within a series of related molecules, the chalcogenoxanthylium dyes **3**–**12** of Scheme 1 were prepared via a similar approach. The Grignard reagents prepared from 3-bromo or 4-bromo derivatives of various substituted benzenes were added to the chalcogenoxanthen-9-ones

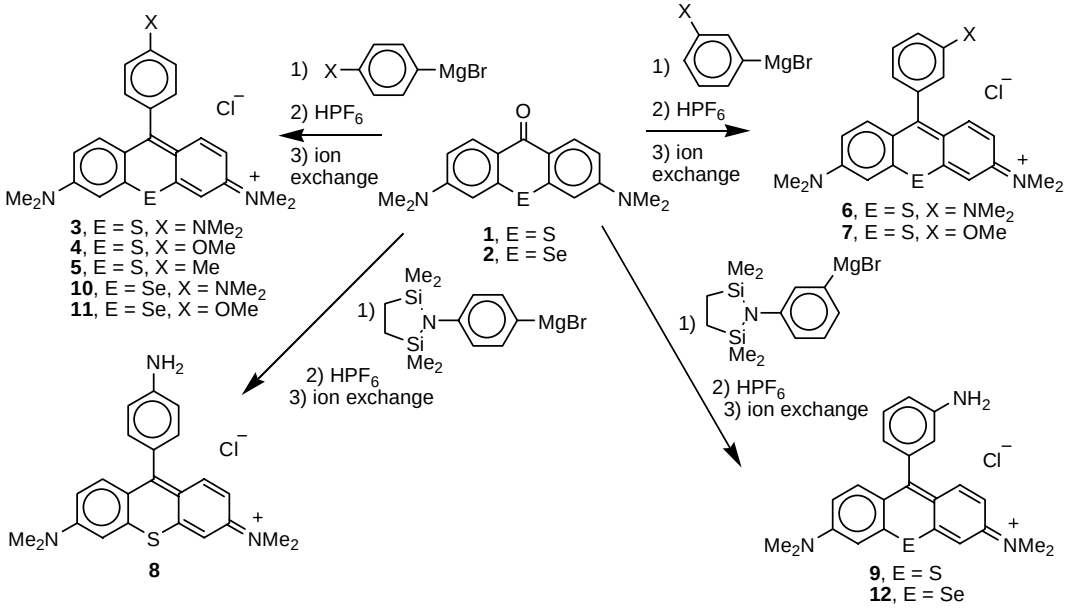

Scheme 1. Synthesis of thio- and seleno-analogues of **TMR**.

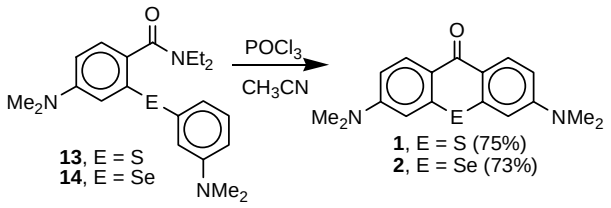

Scheme 2. Synthesis of chalcogenoxanthen-9-one **1** and **2**.

Table 1. Absorption maxima (λ_{max}) and molar extinction coefficients (ε) in MeOH and *n*-octanol/water partition coefficients (log *P*) for **TMR-S**, **TMR-Se**, and **3**–**12**

Compound	E	9-Ph-X	MeOH		log *P*[a]
			λ_{max} (nm)	ε ($M^{-1}cm^{-1}$)	
TMR-S	S	H	571	50,100	0.07 ± 0.02
TMR-Se	Se	H	582	69,200	−0.09 ± 0.09
3	S	4-NMe_2	573	72,400	0.94 ± 0.01
4	S	4-OMe	569	97,700	−0.09 ± 0.03
5	S	4-Me	570	95,400	0.81 ± 0.04
6	S	3-NMe_2	573	72,400	1.13 ± 0.02
7	S	3-OMe	571	87,100	0.14 ± 0.01
8	S	4-NH_2	565	75,800	0.20 ± 0.02
9	S	3-NH_2	571	51,000	0.05 ± 0.03
10	Se	4-NMe_2	576	56,200	0.49 ± 0.02
11	Se	4-OMe	576	56,200	0.18 ± 0.09
12	Se	3-NH_2	582	56,300	−0.37 ± 0.092

[a] pH 6.0 phosphate buffer as the aqueous phase.

1 and **2**.[14,16] Dehydration with AcOH/HPF_6 gave the PF_6^- salts of dyes **3**–**12**. Ion exchange with Amberlite IRA-400 chloride exchange resin gave the chloride salts **3**–**12** in 40–98% isolated yields overall.

The chalcogenoxanthen-9-ones **1** and **2** have been prepared in low yield from benzamide derivatives **13** and **14**, respectively, and strong base.[14,16] We have found that the yields are greatly improved by cyclization with $POCl_3$ in refluxing acetonitrile as shown in Scheme 2. Chalcogenoxanthones **1** and **2** were isolated in 75% and 73% isolated yields, respectively, with this approach.

Values of absorption maxima, λ_{max}, and associated molar extinction coefficients, ε, as well as values of the *n*-octanol/water partition coefficient(log *P*) are compiled in Table 1. Values of λ_{max} are not very sensitive to the nature of the substituent attached to the 9-phenyl substituent on the chalcogenoxanthylium nucleus (Table 1). The range of values of λ_{max} for the thio **TMR** analogues is 565–573 nm, while the range of values for the seleno **TMR** analogues is 576–582 nm.

Values of the *n*-octanol/water partition coefficient, log *P*, are more sensitive to substituent effects with a range from −0.37 for 3-aminophenyl seleno derivative **12** to 1.13 for 3-*N*,*N*-dimethylaminophenyl thio derivative **6**. The *N*,*N*-dimethylamino-substituted derivatives **3**, **6**, and **10** and 4-methylphenyl derivative **5** were the most lipophilic dyes in the series. Methoxy-substituted derivatives **4**, **7**, and **11**, **TMR-S**, **TMR-Se**, and amino-substituted derivatives **8**, **9**, and **12** were far more hydrophilic with values of log *P* near 0.

Quantum yields for the generation of singlet oxygen [$\phi(^1O_2)$] by direct detection of singlet oxygen[17] and quantum yields for fluorescence (ϕ_F) were measured for **3**–**12** in $CHCl_3$ and MeOH and values are summarized in Table 2. Substituents on the 9-phenyl ring had a pronounced effect on values of $\phi(^1O_2)$ and ϕ_F. Values of both $\phi(^1O_2)$ and ϕ_F are low ($\leqslant$0.04) for derivatives containing the *N*,*N*-dimethylamino substituent, presumably due to increased rates of internal conversion in these systems. Even the seleno analogue **10** had a small value of $\phi(^1O_2)$, indicating the intersystem crossing was not competitive with internal conversion in these derivatives. Rates of internal conversion were not as dominant in the amino-substituted derivatives. Values of $\phi(^1O_2)$ were between 0.02 and 0.06 for thio derivatives **8** and **9**, while values of ϕ_F were between 0.01 and 0.09. The 3-aminophenyl seleno derivative **12** gave $\phi(^1O_2)$ of 0.31 in $CHCl_3$.

With **TMR-S**, **TMR-Se**, methoxyphenyl derivatives **4**, **7**, and **11**, and 4-methylphenyl derivative **5**, internal conversion was small relative to the combined yields of $\phi(^1O_2)$ and ϕ_F (Table 2). For the thio derivatives **TMR-S**, **4**, **5**, and **7**, $\phi(^1O_2)$ ranged between 0.09 and 0.30 and ϕ_F ranged between 0.23 and 0.44. For seleno derivatives **TMR-Se** and **11**, $\phi(^1O_2)$ ranged between 0.53 and 0.87, while ϕ_F was $\leqslant$0.01. In general, values of $\phi(^1O_2)$ were higher in $CHCl_3$ relative to MeOH, while values of ϕ_F were slightly higher in MeOH relative to $CHCl_3$.

2.2. Intracellular accumulation of heavy-chalcogen analogues of TMR

As shown in Table 2, thio analogues **TMR-S**, **4**, and **7** were sufficiently fluorescent to allow quantitative determination of cellular uptake into AUXB1 and CR1R12 cells. Drug-sensitive AUXB1 cells or multidrug-resistant CR1R12 cells were exposed to various concentrations of **TMR-S**, **4**, or **7** in the dark for 2 h in complete medium. The data displayed in Figure 1 demonstrate that nearly identical uptake is observed for **TMR-S**, **4**, and **7** in the drug-sensitive AUXB1 cells and that 5–8 femtomole per cell of these dyes is retained by the cells when exposed to 1×10^{-5} M dye for 2 h. Addition of 5×10^{-5} M verapamil prior to dye exposure did not affect the uptake of these dyes into the AUXB1 cells (data not shown).

In contrast, exposure of the multidrug-resistant CR1R12 cells to 1×10^{-5} M **TMR-S**, **4**, or **7** for 2 h gave only 3–4 femtomole per cell as shown in Figure 2. However, when the CR1R12 cells have a 15 min prior exposure to 5×10^{-5} M verapamil, a 2- to 4-fold increase in intracellular dye accumulation was obtained as shown in Figure 2 for dye concentrations of 1×10^{-6} to 1×10^{-5} M.

The data in Figure 2 demonstrate that uptake of **TMR-S** or dye **4** in CR1R12 cells is significantly greater for all the concentrations tested than the uptake of compound **7**. *P* values range from <0.05 to <0.001 for

Table 2. Quantum yields for the generation of singlet oxygen [$\phi(^1O_2)$] and for fluorescence (ϕ_F) in MeOH and $CHCl_3$ for **TMR-S**, **TMR-Se**, and **3–12**

Compound	9-Ph-X	$\phi(^1O_2)$		ϕ_F	
		MeOH[a]	$CHCl_3$[a]	MeOH[a]	$CHCl_3$[a]
TMR-S	H	0.21 ± 0.01[b]	—	0.44 ± 0.01[b]	—
TMR-Se	H	0.87 ± 0.02[b]	—	0.005 ± 0.01[b]	—
3	4-NMe_2	0.01 ± 0.01	0.01 ± 0.01	0.003 ± 0.001	0.003 ± 0.001
4	4-OMe	0.09 ± 0.01	0.22 ± 0.01	0.27 ± 0.01	0.23 ± 0.01
5	4-Me	0.11 ± 0.01	0.26 ± 0.01	0.29 ± 0.01	0.23 ± 0.01
6	3-NMe_2	0.02 ± 0.01	0.04 ± 0.01	0.001 ± 0.001	0.001 ± 0.001
7	3-OMe	0.16 ± 0.02	0.30 ± 0.02	0.35 ± 0.02	0.28 ± 0.02
8	4-NH_2	0.02 ± 0.01	0.05 ± 0.01	0.04 ± 0.01	0.07 ± 0.01
9	3-NH_2	0.04 ± 0.01	0.06 ± 0.01	0.01 ± 0.01	0.09 ± 0.02
10	4-NMe_2	0.02 ± 0.01	0.02 ± 0.01	0.001 ± 0.001	0.001 ± 0.001
11	4-OMe	0.60 ± 0.02	0.53 ± 0.02	0.01 ± 0.01	0.01 ± 0.01
12	3-NH_2	0.05 ± 0.01	0.31 ± 0.01	0.004 ± 0.001	0.004 ± 0.001

[a] ±standard deviation.
[b] Ref. 14.

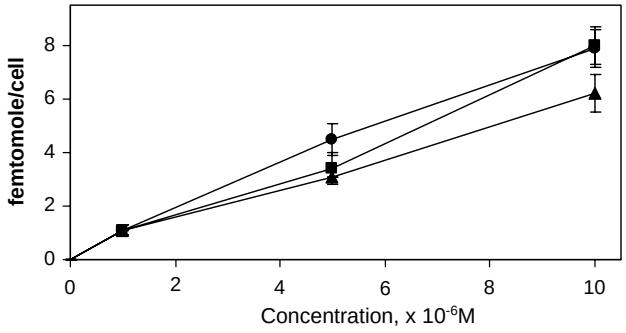

Figure 1. Intracellular accumulation of **TMR-S** (■) and thio derivatives **4** (●) or **7** (▲) with methoxy substituents into drug sensitive AUXB1 cells. Cell culture and dye exposure conditions and the method to determine the intracellular dye content are described in detail in Section 4. Each data point represents the mean obtained from at least three separate experiments performed in duplicate, error bars are the SEM.

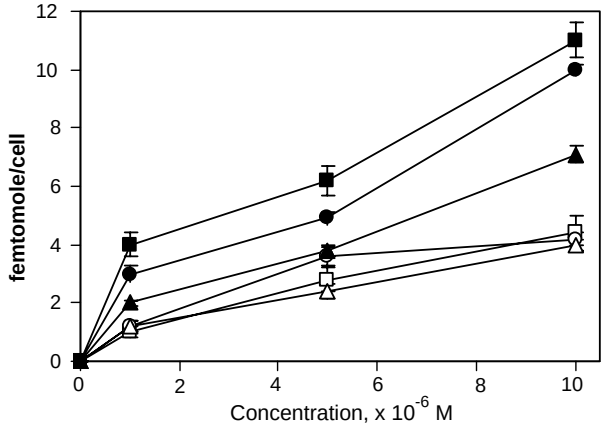

Figure 2. Intracellular accumulation of **TMRS** (□), **4** (○) or **7** (△) into cultured multidrug resistant CR1R12 cells and intracellular accumulation of **TMRS** (■), **4** (●) or **7** (▲) in cells exposed to 5×10^{-5} M verapamil prior to addition of dyes to cell monolayers. Cell culture and dye exposure conditions and the method to determine the intracellular dye content are described in detail in Section 4. Each data point represents the mean obtained from at least three separate experiments performed in duplicate, error bars are the SEM.

the comparisons. It is interesting to note that uptake of **TMR-S**, **4**, and **7** into CR1R12 cells after exposure to 5×10^{-5} M verapamil is equivalent to or marginally greater than the uptake of these dyes into the drug-sensitive AUXB1 cells (Fig. 1 vs. Fig. 2).

2.3. Phototoxicity of thio-analogues of TMR towards AUXB1 and CR1R12 cells

To compare the phototoxicity of the heavy-chalcogen analogues of **TMR**, cultured chemosensitive AUXB1 and multidrug-resistant CR1R12 cells were exposed to the compounds for 2 h in the dark and then irradiated with 5 J cm^{-2} broad band, 350–750 nm visible light. Dark controls were treated with dye for 2 h and not irradiated. The CR1R12 cells were treated with 5×10^{-5} M verapamil for 15 min prior to treatment with the thio analogues of **TMR**. The data shown in Figure 3 depict the results obtained from chemosensitive AUXB1 cells that were exposed to **TMR-S** and the thiotetramethylrosamine analogues **3–9**. In the absence of light, **TMR-S** and **3–9** gave >90% cell survival in AUXB1 cells at concentrations up to 1×10^{-5} M with or without added verapamil (data not shown). The data obtained demonstrate that **TMR-S** and 4-tolyl derivative **5** were the two most phototoxic compounds with nearly identical phototoxicity toward AUXB1 cells and were phototoxic at all the concentrations tested. 4-Methoxyphenyl derivative **4** was the next most effective photosensitizer and was significantly more phototoxic than 3-methoxyphenyl derivative **7** at lower dye concentrations. However, all four of these compounds have equivalent phototoxicity at or above 1×10^{-6} M. Derivative **3** is only phototoxic at concentrations of 1×10^{-6} M or higher. Analogues **6**, **8**, and **9** demonstrated little or no phototoxicity toward AUXB1 cells at any concentration. These data indicate that, at least at lower concentrations, substituent effects impact phototoxicity in the thio-tetramethylrosamine derivatives.

In the absence of prior exposure to verapamil, none of the thio analogues of **TMR** showed any significant dark or phototoxicity (>90% cell survival) toward CR1R12

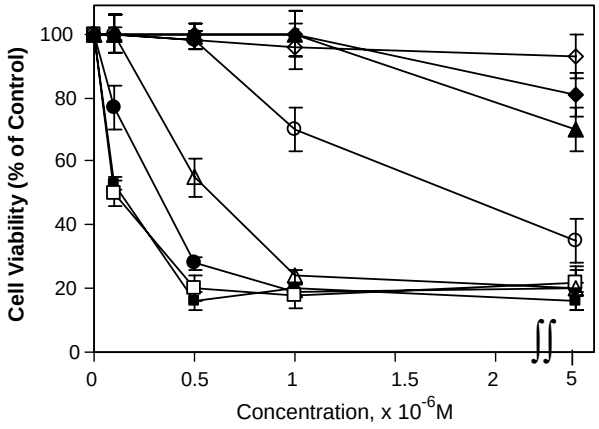

Figure 3. Phototoxicity of **TMR-S** and thio-tetramethylrosamine analogues **3**–**9** towards chemosensitive AUXB1 cells. The data depict the results obtained after chemosensitive AUXB1 cells were exposed to **TMR-S** (■), **3** (○), **4** (●), **5** (□), **6** (▲), **7** (△), **8** (◊), or **9** (♦). Cell culture and dye and light exposure conditions are described in detail in Section 4. Each data point represents the mean of at least three separate experiments performed in duplicate, error bars are the SEM. Data are expressed as percent cell viability compared to control cells, those exposed to neither dye nor light.

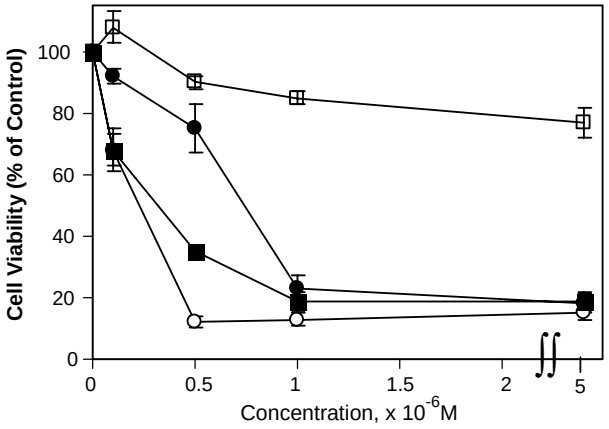

Figure 5. A comparison of the phototoxicity of **TMR-Se** (○) and seleno-tetramethylrosamine analogues **10** (●), **11** (■), and **12** (□). Cell culture and dye and light exposure conditions are described in detail in Section 4. Each data point represents the mean of at least three separate experiments performed in duplicate, error bars are the SEM. Data are expressed as percent cell viability compared to control cells, those exposed to neither dye nor light.

cells at concentrations $\leqslant 5 \times 10^{-6}$ M (data not shown). If the CR1R12 cells were treated with 5×10^{-5} M verapamil for 15 min prior to treatment with the photosensitizers, then substituent effects impacted photosensitizer potency. In the CR1R12 cells, none of the aminophenyl- or *N*,*N*-dimethylaminophenyl-substituted compounds—**3**, **6**, **8**, and **9**—showed any phototoxicity. However, the phototoxicity of **TMR-S** and the methoxy-substituted derivatives **4** and **7** toward these cells (Fig. 4) was consistent with their rank order of uptake: **TMR-S > 4 > 7**, as shown in Figure 2. Derivative **5** was identical to **TMR-S** with respect to phototoxicity toward CR1R12 cells. In the presence of 5×10^{-5} M verapamil and in the absence of light, **TMR-S** and **3**–**9** gave >90% cell survival in CR1R12 cells at concentrations up to 1×10^{-5} M (data not shown). Comparison of cell viability following treatment of either AUXB1 or CR1R12 cells with **TMR-S**, **4**, **5**, or **7** and 5 J cm^{-2} of 350–750 nm light suggests that AUXB1 cells are more susceptible to photodamage than CR1R12 cells.

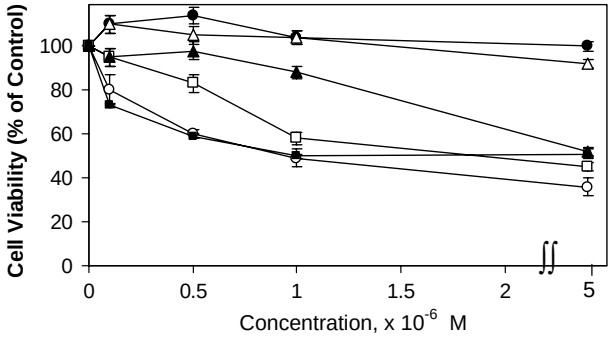

Figure 4. Phototoxicity of **TMR-S** (○), **3** (●), **4** (□), **5** (■), **6** (△), or **7** (▲) towards multidrug resistant CR1R12 cells following a 15-min incubation with 5×10^{-5} M verapamil. Cell culture and dye and light exposure conditions are described in detail in Section 4. Each data point represents the mean of at least three separate experiments performed in duplicate, error bars are the SEM. Data are expressed as percent cell viability compared to control cells, those exposed to neither dye nor light.

2.4. Phototoxicity of selenium-containing TMR analogues towards chemosensitive AUXB1 cells

The selenotetramethylrosamine analogues—**TMR-Se**, **10** with a 4-*N*,*N*-dimethylaminophenyl substituent, **11** with a 4-methoxyphenyl substituent, and **12** with a 3-aminophenyl substitutent—were tested for their phototoxicity toward chemosensitive AUXB1 cells with the data shown in Figure 5. **TMR-Se** and **TMR-S** (Fig. 3) displayed nearly identical phototoxicity as did thio analogue **4** (Fig. 3) and its seleno analogue **11** toward AUXB1 cells. The chalcogen atom had little impact on phototoxicity in spite of its impact on the values of ϕ ($^1O_2$) for **TMR-S**, **TMR-Se**, **4**, and **11** and related compounds. In the absence of light, none of these derivatives showed significant dark toxicity (>90% cell survival) at concentrations up to 1×10^{-5} M.

3. Discussion

A variety of substituents are readily introduced at the 9-position of the 2,7-bis-*N*,*N*-dimethylaminoxanthylium core via the addition of aryl Grignard reagents to the chalcogenoxanthone precursors **1** and **2**. The simplest analogues in the series are **TMR-S** and **TMR-Se**—the thio and seleno analogues of **TMR**. From the data in Table 1, the aryl substituents have little impact on wavelengths of absorption and the absorption maxima are dictated by the chalcogen atom. The thio-**TMR** analogues have values of λ_{max} near 570 nm, while the seleno-**TMR** analogues have values of λ_{max} near 580 nm. The 9-aryl substituents do impact values of log *P*, the *n*-octanol/water partition coefficient.

The 9-aryl substituents exert a strong influence on photophysical properties. The dominant features of the excited state photophysics are fluorescence, intersystem crossing to the triplet, which can then generate singlet oxygen, and internal conversion. The *N*,*N*-dimethylamino group markedly increases internal conversion at the expense of fluorescence and intersystem crossing to the triplet (Table 2). The 9-phenyl substituent, 9-4-methylphenyl substituent, 9-4-methoxyphenyl substituent, and 9-3-methoxyphenyl substituent appear to have much smaller contributions from internal conversion. The excited state photophysics for molecules containing these groups is dominated by fluorescence and intersystem crossing for the thio analogues as reflected in values of ϕ_F and $\phi(^1O_2)$ and by intersystem crossing for the seleno analogues as reflected in values of $\phi(^1O_2)$ (Table 2).

The data expressed in Figures 3 and 5 can be extrapolated to give the effective concentrations for 50% cell kill with 5 J cm^{-2} of 350–750 nm light (EC_{50}) for AUXB1 cells and, from Figure 4, the EC_{50} for CR1R12 cells. These values, while approximate, are compiled in Table 3. On the basis of the EC_{50} values, the rank order of photosensitizer efficiency toward AUXB1 cells is **TMR-S** ≈ **5** > **TMR-Se** > **4** ≈ **11** > **7** > **3** with **6**, **8**, **9**, and **12** showing essentially no phototoxicity at 5×10^{-6} M. The corresponding rank order for values of $\phi(^1O_2)$ is **TMR-Se** > **11** > **TMR-S** ≈ **7** > **5** > **4** > **3**, which suggests that photosensitizer potency is not a simple function of $\phi(^1O_2)$. Toward CR1R12 cells, the rank order of potency is **TMR-S** ≈ **5** > **4** > **7** with **3** and **6** showing essentially no phototoxicity at 5×10^{-6} M.

For AUXB1 cells, the uptake of **TMR-S**, **4**, and **7** is identical, suggesting that the 7-fold differences in values of EC_{50} are due to factors other than uptake and photophysical differences. In the CR1R12 cells, the phototoxicity and uptake appear to be directly correlated for **TMR-S**, **4**, and **7**, which may relate to the propensity of these materials to be transported by Pgp.

From values of $\phi(^1O_2)$ summarized in Table 2, **TMR-Se** is far more efficient than either **TMR-S** or **5** for the generation of singlet oxygen, yet all three of these molecules have similar potency as photosensitizers. Furthermore, values of log *P* are nearly identical for **TMR-S** and **TMR-Se** (0.07 and −0.09, respectively) and these two molecules are far more hydrophilic than thio derivative **5** (log *P* of 0.81, Table 1). Consequently, phototoxicity does not appear to be a function of lipophilicity. Another pair of interesting comparisons is found in the 4-*N*,*N*-dimethylaminophenyl-substituted derivatives **3** and **10**. As shown in Table 2, values of $\phi(^1O_2)$ are low and nearly identical for these two molecules in solution yet seleno analogue **10** has an EC_{50} of 0.7 times 10^{-6} M toward AUXB1 cells, while EC_{50} for **3** is 4×10^{-6} M. Both of these molecules are more lipophilic than **TMR-S** and **TMR-Se**. Clearly, the photosensitizer performance is not simply a function of either log *P* or $\phi(^1O_2)$.

These data, taken together, demonstrate that substituent effects among the various thio and selenotetramethylrosamine analogues impact phototoxicity toward either AUXB1 or CR1R12 cells. In the CR1R12 cells, the addition of verapamil enhances the uptake of the various photosensitizers and the relative phototoxicity of **TMR-S**, **4**, **5**, and **7** in both AUXB1 and CR1R12 cells follow the same trend **TMR-S** ≈ **5** > **4** > **7**.

In an earlier report, we demonstrated that photosensitization of Pgp-expressing CR1R12 cells by **TMR-S** and **TMR-Se** enhanced the uptake of the Pgp transport molecule Calcein AM, indicating that these analogues do impact the function of this drug efflux pump.[15] The data presented here demonstrate that substituent effects among the various thio and selenotetramethylrosamine analogues impact their phototoxicity toward either chemosensitive AUXB1 cells or multidrug-resistant CR1R12 cells. The substituent effects for the **TMR** analogues were realized in drug-resistant CR1R12 cells only when the Pgp modulator verapamil was present indicating that the substituent effects extend to the interaction between the chemical structure of the analogues and binding/transport function of Pgp.

Table 3. Concentrations of photosensitizers **TMR-S**, **TMR-Se**, and **3**–**12** to give 50% cell kill (EC_{50}) of AUXB1 or CR1R12 cells with 5 J cm^{-2} of 350–750 nm light

Compound	E	9-Ph-X	$EC_{50} \times 10^6$		
			M(AUXB1)	M(CR1R12)	$\phi(^1O_2)$, MeOH[a]
TMR-S	S	H	0.1	1.0	0.21[b]
TMR-Se	Se	H	0.2	—	0.87[b]
3	S	4-NMe_2	4.0	>5.0	0.01
4	S	4-OMe	0.3	2.0	0.09
5	S	4-Me	0.1	1.0	0.11
6	S	3-NMe_2	>5.0	>5.0	0.02
7	S	3-OMe	0.7	5.0	0.16
8	S	4-NH_2	>5.0	—	0.02
9	S	3-NH_2	>5.0	—	0.04
10	Se	4-NMe_2	0.7	—	0.02
11	Se	4-OMe	0.3	—	0.60
12	Se	3-NH_2	>5.0	—	0.05

[a] See Table 2 for standard deviation.

4. Experimental

4.1. General methods

All the chemicals and reagents were purchased from Sigma Chemical Co. (St. Louis, MO, USA) unless otherwise noted. Cell culture media and antibiotics were obtained from Grand Island Biological (Grand Island, NY, USA). Fetal bovine serum (FBS) was purchased from Atlanta Biologicals (Atlanta, GA, USA).

4.1.1. General procedure for the preparation of chalcogenoxanthylium dyes: preparation of 2,7-bis-*N*,*N*-dimethylamino-9-(4-*N*,*N*-dimethylaminophenyl)thioxanthylium chloride (3). A mixture of *N*,*N*-dimethyl-4-bromoaniline (0.50 g, 2.5 mmol) and ground magnesium turnings (0.060 g, 2.5 mmol) in 5 mL of anhydrous THF was heated at reflux for 2 h and then cooled to ambient temperature. The resulting solution was then added to a solution of thioxanthenone **1** (0.140 g, 0.47 mmol) in anhydrous THF (5 mL). The reaction mixture was heated at reflux for 1.5 h, cooled to ambient temperature and then to 0 °C. Following this, acetic acid (3.0 mL) was added. Hexafluorophosphoric acid (60% by-weight solution in water) was added dropwise until a color change was observed. Ice water (50 mL) was added and the resulting precipitate was filtered. The precipitate was dissolved in a 50/50 mixture of ethanol/acetonitrile and stirred with Amberlite IRA-400 chloride exchange resin (0.500 g) for 1 h. The resin was removed by filtration and the ion exchange was repeated with fresh resin (2x). The solvent was removed and the resulting solid was recrystallized from acetonitrile/ether to yield 0.164 mg (80%) of **3** as a dark purple solid, mp >300 °C. ^{1}H NMR (500 MHz, CD_3CN) δ 7.55 (d, 2H, J = 9.5 Hz), 7.19 (d, 2H, J = 8.5 Hz), 7.17 (2, 2H, J = 2.5 Hz), 7.00 (d × d, 2H, J = 2.5, 9.5 Hz), 6.93 (2, 2H, J = 9 Hz), 3.21 (s, 12H), 3.06 (s, 6H); ^{13}C NMR (75.5 MHz, CD_3CN) δ 160.6, 154.4, 152.3, 144.9, 137.5, 132.0, 123.4, 120.2, 116.0, 112.4, 106.4, 40.9, 40.5; HRMS (ES) m/z 402.2005 (calcd for $C_{25}H_{28}N_3S^+$: 402.1998); λ_{max} (CH_2Cl_2) 564 nm ($\varepsilon = 1.00 \times 10^5$ $M^{-1}cm^{-1}$), λ_{max} (CH_3OH) 565 nm ($\varepsilon = 1.05 \times 10^5$ $M^{-1}cm^{-1}$). Anal. Calcd for $C_{25}H_{28}N_3SCl$: C, 68.55; H, 6.44; N, 9.59. Found: C, 68.57; H, 6.31; N, 9.61.

4.1.2. Preparation of 2,7-bis-*N*,*N*-dimethylamino-9-(4-methoxyphenyl)thioxanthylium chloride (4). 4-Bromoanisole (0.935 g, 5.0 mmol), ground magnesium turnings (0.12 g, 5.0 mmol), and thioxanthen-9-one **1** (0.10 g, 0.34 mmol) were treated as described. Following the final ion exchange, the filtrate was concentrated and the crude chloride salt was recrystallized from acetonitrile/ether to give 0.10 g (70%) of **4** as a dark purple solid, mp >300 °C. ^{1}H NMR (400 MHz, CD_3CN) δ 7.42 (d, 2H, J = 9.6 Hz), 7.27 (d, 2H, J = 8.8 Hz), 7.20 (d, 2H, J = 2.4 Hz), 7.17 (d, 2H, J = 8.8 Hz), 6.99 (d × d, 2H, J = 2.4, 9.6 Hz), 3.91 (s, 3H), 3.21 (s, 12H); ^{13}C NMR (75.5 MHz, CD_3CN) δ 161.6, 161.3, 154.6, 145.1, 137.3, 131.8, 128.7, 120.2, 116.3, 115.1, 106.6, 56.3, 41.0; HRMS (ES) m/z 389.1684 (calcd for $C_{24}H_{25}N_2OS^+$: 389.1682); λ_{max} (CH_2Cl_2) 569 nm ($\varepsilon = 1.10 \times 10^4$ $M^{-1}cm^{-1}$), λ_{max} (CH_3OH) 569 nm ($\varepsilon = 9.8 \times 10^4$ $M^{-1}cm^{-1}$). Anal. Calcd for $C_{24}H_{25}N_2OSCl$: C, 67.83; H, 5.93; N, 6.59. Found: C, 67.68; H, 6.04; N, 6.47.

4.1.3. Preparation of 2,7-bis-*N*,*N*-dimethylamino-9-(4-methylphenyl)thioxanthylium chloride (5). *p*-Tolylmagnesiumbromide (1.34 mL, 1.3 mmol, 1 M solution in ether) and thioxanthen-9-one **1** (0.10 g, 0.34 mmol) were treated as described. Following the final ion exchange, the crude chloride salt was recrystallized from acetonitrile/ether to give 0.136 g (98%) of **5** as a dark purple solid, mp >300 °C. ^{1}H NMR (400 MHz, CD_3CN) δ 7.45 (d, 2H, J = 8.0 Hz), 7.36 (d, 2H, J = 10 Hz), 7.23 (d, 2H, J = 8.0 Hz), 7.20 (d, 2H, J = 2.8 Hz), 6.98 (d × d, 2H, J = 2.8, 10 Hz), 3.21 (s, 12H), 2.49 (s, 3H); ^{13}C NMR (125.5 MHz, CD_3CN) δ 161.3, 154.4, 145.0, 140.6, 137.1, 133.8, 130.2, 130.1, 119.9, 116.3, 106.5, 41.0, 21.4; HRMS (ES) m/z 373.1736 (calcd for $C_{24}H_{25}N_2S^+$: 373.1738); λ_{max} (CH_2Cl_2) 569 nm, ($\varepsilon = 13.1 \times 10^4$ $M^{-1}cm^{-1}$); λ_{max} (CH_3OH) 570 nm ($\varepsilon = 9.5 \times 10^4$ $M^{-1}cm^{-1}$). Anal. Calcd for $C_{24}H_{25}N_2SCl$: C, 67.83; H, 5.93; N, 6.59. Found: C, 67.84; H, 5.86; N, 6.62.

4.1.4. Preparation of 2,7-bis-*N*,*N*-dimethylamino-9-(3-*N*,*N*-dimethylaminophenyl)thioxanthylium chloride (6). *N*,*N*-Dimethyl-3-bromoaniline (0.50 g, 2.5 mmol), ground magnesium turnings (0.060 g, 2.5 mmol), and thioxanthen-9-one **1** (0.14 g, 0.47 mmol) were treated as described. The crude chloride salt was recrystallized from acetonitrile and a small amount of ether to give 0.154 g (75%) of **10** as a dark green solid, mp >300 °C. ^{1}H NMR (500 MHz, CD_3OD) δ 7.62 (t, 1H, J = 8.0 Hz), 7.52 (d, 2H, J = 9.5 Hz), 7.38–7.32 (m, 3H), 7.14 (d × d, 2H, J = 2.5, 9.5 Hz), 7.08 (br s, 1H), 6.98 (br s, 1H), 4.91 (s, 12H), 3.15 (s, 6H); ^{13}C NMR (75.5 MHz, 50/50 CD_3OD/CD_2Cl_2) δ 160.8, 154.5, 148.7, 145.3, 137.8, 137.2, 130.7, 123.0, 119.8, 116.9 (2C), 116.1, 106.2, 42.9, 40.8; HRMS (ES) m/z 402.1996 (calcd for $C_{25}H_{28}N_3S^+$: 402.1998); λ_{max} (CH_2Cl_2) 573 nm ($\varepsilon = 1.09 \times 10^5$ $M^{-1}cm^{-1}$), λ_{max} (CH_3OH) 573 nm, ($\varepsilon = 7.3 \times 10^4$ $M^{-1}cm^{-1}$). Anal. Calcd for $C_{25}H_{28}N_3SCl$: C, 68.55; H, 6.44; N, 9.59. Found: C, 68.19; H, 6.51; N, 9.41.

4.1.5. Preparation of 2,7-bis-*N*,*N*-dimethylamino-9-(3-methoxyphenyl)thioxanthylium chloride (7). 3-Bromoanisole (0.935 g, 5.0 mmol), ground magnesium turnings (0.12 g, 5.0 mmol), and thioxanthen-9-one **1** (0.10 g, 0.34 mmol) were treated as described. Following the final ion exchange, the crude chloride salt was recrystallized from acetonitrile/ether to give 0.070 g (40%) of **7** as a dark purple solid, mp >300 °C. ^{1}H NMR (400 MHz, CD_3CN) δ 7.54 (t, 1H, J = 8.2 Hz), 7.39 (d, 2H, J = 9.6 Hz), 7.22 (d, 2H, J = 2.4 Hz), 7.18 (d × d × d, 1H, J = 1.0, 2.6, 8.2 Hz), 6.99 (d × d, 2H, J = 9.6, 2.4 Hz), 6.93–6.91 (m, 2H), 3.82 (s, 3H), 3.22 (s, 12H); ^{13}C NMR (75.5 MHz, CD_3CN) δ 160.7, 160.5, 154.5, 145.1, 138.1, 137.1, 130.9, 122.4, 119.6, 116.4, 116.0, 115.6, 106.7, 56.2, 41.1; HRMS (ES) m/z 389.1684 (calcd for $C_{24}H_{25}N_2OS^+$: 389.1682); λ_{max} (CH_2Cl_2) 572 nm ($\varepsilon = 9.6 \times 10^4$ $M^{-1}cm^{-1}$), λ_{max}

(CH_3OH) 571 nm ($\varepsilon = 8.7 \times 10^4$ $M^{-1}cm^{-1}$). Anal. Calcd for $C_{24}H_{25}N_2OSCl$: C, 67.83; H, 5.93; N, 6.59. Found: C, 67.76; H, 5.91; N, 6.71.

4.1.6. Preparation of 2,7-bis-*N*,*N*-dimethylamino-9-(4-aminophenyl)thioxanthylium chloride (8). 1-(4-Bromophenyl)-2,2,5,5-tetraethyl-1,2,5-azadisilolidine (0.50 g, 1.6 mmol), magnesium turnings (0.040 g, 1.7 mmol), and thioxanthen-9-one **1** (0.119 g, 0.40 mmol) were treated as described. Following the final ion exchange, the the crude chloride salt was recrystallized from CH_3CN/ether to give 0.095 g (58 %) of a dark green solid, mp > 300 °C. ^1H NMR (500 MHz, CD_3OD) δ 7.68 (d, 2H, $J = 10$ Hz), 7.30 (d, 2H, $J = 2.5$ Hz), 7.12 (d × d, 2H, $J = 2.5$, 10 Hz), 7.09 (d, 2H, $J = 8$ Hz), 6.91 (d, 2H, $J = 8$ Hz), 3.29 (s, 12H); ^{13}C NMR (75.5 MHz, CD_2Cl_2) δ 153.80, 144.74, 137.44, 131.46, 120.07, 115.29, 114.71, 105.66, 40.84; λ_{max} (CH_3OH) 565 nm ($\varepsilon = 7.63 \times 10^4$ M^{-1} cm^{-1}); HRMS (ESI) *m/z* 374.1697 (Calcd for $C_{23}H_{24}N_3S^+$: 374.1685). Anal. Calcd for $C_{23}H_{24}N_3SCl$: C, 67.38; H, 5.90; N, 10.25. Found: C, 67.22; H, 5.95; N, 10.26.

4.1.7. Preparation of 2,7-bis-*N*,*N*-dimethylamino-9-(3-aminophenyl)thioxanthylium chloride (10). 1-(3-Bromophenyl)-2,2,5,5-tetraethyl-1,2,5-azadisilolidine (0.50 g, 1.6 mmol), magnesium turnings (0.040 g, 1.7 mmol), and thioxanthen-9-one **1** (0.119 g, 0.40 mmol) were treated as described. Following the final ion exchange, the crude chloride was recrystallized from acetonitrile and a small amount of diethyl ether to give 0.088 g (54%) of the product as a dark green solid, mp > 300 °C. ^1H NMR (500 MHz, CD_3OD) δ 7.64 (t, 1H, $J = 7.5$, 8.5 Hz), 7.45 (d, 2H, $J = 9.5$ Hz), 7.38 (m, 1H), 7.36 (d, 2H, $J = 2.5$ Hz), 7.15 (m, 2H), 7.12 (d × d, 2H, $J = 2.5$, 9.5 Hz), 3.31 (s, 12H); ^{13}C NMR (125 MHz, CD_3OD, 45 °C) δ 160.9, 155.3, 145.8, 138.5, 137.5, 137.4, 131.2, 131.1, 124.4, 120.3, 120.0, 116.7, 106.8, 40.7; λ_{max} (MeOH) 571 nm ($\varepsilon = 3.04 \times 10^4$ M^{-1} cm^{-1}); HRMS (ESI) *m/z* 374.1695 (Calcd for $C_{23}H_{24}N_3S^+$: 374.1685). Anal. Calcd for $C_{23}H_{24}N_3SCl$: C, 67.38; H, 5.90; N, 10.25. Found: C, 67.05; H, 6.01; N, 10.04.

4.1.8. Preparation of 2,7-bis-*N*,*N*-dimethylamino-9-(4-*N*,*N*-dimethylaminophenyl)selenoxanthylium chloride (10). *N*,*N*-Dimethyl-4-bromoaniline (0.23 g, 1.2 mmol), ground magnesium turnings (0.030 g, 1.2 mmol), and selenoxanthen-9-one **2** (0.10 g, 0.29 mmol) were treated as described. Following the final ion exchange, the crude chloride salt was recrystallized from CH_3CN and a small amount of ether to give 0.089 g (69 %) of **10** as a dark green solid, mp 251–252 °C. ^1H NMR (500 MHz, CD_2Cl_2)δ 7.68 (d, 2H, $J = 9.8$ Hz), 7.24 (d, 2H, $J = 2.4$ Hz), 7.14 (d, 2H, $J = 8.5$ Hz), 6.87 (d, 2H, $J = 8.5$ Hz), 6.84 (d × d, 2H, $J = 2.4$, 9.8 Hz), 3.24 (s, 12H), 3.09 (s, 6H); ^{13}C NMR (125 MHz, CD_2Cl_2) δ 153.5, 144.4, 136.5, 135.4, 129.5, 129.2, 128.7, 119.2, 115.1, 114.2, 105.4, 40.5; λ_{max} (CH_2Cl_2) 576 nm ($\varepsilon = 5.6 \times 10^4$ M^{-1} cm^{-1},) 580 nm (sh, $\varepsilon = 5.7 \times 10^3$ M^{-1} cm^{-1}); HRMS (ESI) *m/z* 450.1440 (Calcd for $C_{25}H_{28}N_3{}^{80}Se$: 450.1443). Anal. Calcd for $C_{25}H_{28}N_3SeCl$: C, 61.92; H, 5.82; N, 8.67. Found: C, 61.83; H, 5.95; N, 8.47.

4.1.9. Preparation of 2,7-bis-*N*,*N*-dimethylamino-9-(4-methoxyphenyl) selenoxanthylium chloride (11). 4-Bromoanisole (1.62 g, 17.0 mmol), ground magnesium turnings (0.22 g, 8.0 mmol), and selenoxanthen-9-one **2** (0.15 g, 0.43 mmol) were treated as described. Following the final ion exchange, the crude chloride salt was recrystallized from acetonitrile/ether to give 0.12 g (70%) of **10** as a black solid, mp 245–246 °C. ^1H NMR (500 MHz, CD_2Cl_2) δ 7.51 (d, 2H, $J = 9.8$ Hz), 7.45 (d, 2H, $J = 2.7$ Hz), 7.21 (d × d, 2H, $J = 1.8$, 6.7 Hz), 7.11 (d × d, 2H, $J = 1.8$, 6.7 Hz), 6.83 (d × d, 2H, $J = 2.7$, 9.8 Hz), 3.26 (s, 12H), 2.92 (s, 3H); ^{13}C NMR (75.5 MHz, $CDCl_3$) δ 157.4, 148.9, 134.3, 130.9, 130.0, 128.6, 128.1, 126.5, 113.5, 112.9, 111.6, 54.8, 40.7; λ_{max} (CH_2Cl_2) 576 nm ($\varepsilon = 5.6 \times 10^4$ M^{-1} cm^{-1}), 578 nm, (sh, $\varepsilon = 1.7 \times 10^3$ M^{-1} cm^{-1}); HRMS (ESI) *m/z* 437.1133 (Calcd for $C_{24}H_{25}N_2$ $O^{80}Se^+$: 437.1127). Anal. Calcd for: C, 61.09; H, 5.34; N, 5.94. Found: C, 60.94; H, 5.48; N, 5.95.

4.1.10. Preparation of 2,7-bis-*N*,*N*-dimethylamino-9-(3-aminophenyl)selenoxanthylium chloride (12). 1-(3-Bromophenyl)-2,2,5,5-tetraethyl-1,2,5-azadisilolidine (0.50 g, 1.6 mmol), magnesium turnings (0.040 g, 1.7 mmol), and selenoxanthen-9-one **2** (0.14 g, 0.40 mmol) were treated as described. Following the final ion exchange, the crude chloride was recrystallized from CH_3CN and a small amount of diethyl ether to give 0.070 g (17 %) of the product as a dark green solid, mp 291–292 °C. ^1H NMR (500 MHz, CD_2Cl_2)δ 7.66 (d, 2H, $J = 9.8$ Hz), 7.48 (d, 2H, $J = 2.1$ Hz), 7.35 (t, 1H, $J = 7.5$ Hz), 6.92 (d × d, 1H, $J = 1.5$, 7.4 Hz), 6.87 (d × d, 2H, J = 2.1, 9.8 Hz), 6.74 (d × d, 1H, $J = 1.5$ Hz), 6.62 (d, 1H, $J = 7.6$ Hz) 4.50 (br s, 2H), 3.29 (s, 12H); ^{13}C NMR (300 MHz, CD_3OD) δ 154.7, 147.2, 139.7, 139.6, 130.7, 122.0, 120.7, 118.6, 118.4, 116.1, 110.0, 40.7; λ_{max} (CH_3OH) 582 nm ($\varepsilon = 5.6 \times 10^4$ M^{-1} cm^{-1}); λ_{max} (CH_2Cl_2) = 582 nm, ($\varepsilon = 3.7 \times 10^3$ M^{-1} cm^{-1}); HRMS (ESI) *m/z* 422.1142 (Calcd for $C_{23}H_{24}N_3{}^{80}Se^+$: 422.1130). Anal. Calc for $C_{23}H_{24}N_3SeCl$: C, 60.46; H, 5.29; N, 9.20. Found: C, 60.22; H, 5.51; N, 8.99.

4.1.11. Preparation of 1-(4-bromophenyl)-2,2,5,5-tetramethyl-1,2,5-azadisilolidine[18]. 4-Bromoanaline (1.00 g, 5.81 mmol), triethylamine (1.62 mL, 11.6 mmol) and 4-(dimethylamino)pyridine (0.070 g, 0.58 mmol) were dissolved in CH_2Cl_2 (20 mL) at ambient temperature. 1,2-bis(chlorodimethylsilyl)ethane (1.25 g, 5.81 mmol) in 5 mL of CH_2Cl_2 was added slowly and the resulting mixture was stirred for 3 h. Upon completion, hexanes (30 ml) were added to the reaction mixture precipitating triethylammonium chloride that was removed by filtration. The resulting pale yellow oil was purified by column chromatography on basic alumina, eluted with petroleum ether/ethyl acetate (4/1) to give the stabase-protected aniline in 1.66 g (91%) isolated yield: ^1H NMR ($CDCl_3$) δ 7.34 (AA′BB′, 2H, $J = 8.5$ Hz), 6.84 (AA′BB′, 2H, $J = 8.5$ Hz), 0.91 (s, 4H), 0.25 (s, 12H).

4.1.12. Preparation of 1-(3-bromophenyl)-2,2,5,5-tetramethyl-1,2,5-azadisilolidine[18]. 3-Bromoanaline (1.00 g, 5.81 mmol), triethylamine (1.62 mL, 11.6 mmol), 4-(dimethylamino)pyridine (0.070 g, 0.58 mmol), and 1,2-

bis(chlorodimethylsilyl)ethane (1.25 g, 5.81 mmol) were treated as described to give 1.66 g (93%) of a pale yellow oil: ^{1}H NMR ($CDCl_3$) δ 7.34 (AA′BB′, 2H, J = 8.5 Hz), 6.81 (AA′BB′, 2H, J = 8.5 Hz), 0.91 (s, 4H), 0.25 (s, 12H).

4.1.13. Preparation of bis-2,7-*N*,*N*-dimethylaminothioxanthen-9-one (1). Phosphorus oxychloride (2.7 mL, 29 mmol) and arylthiobenzamide **13** (1.08 g, 2.9 mmol) were heated at reflux in 50 mL of acetonitrile for 1.5 h and the reaction mixture was then poured into a mixture of 75 mL of 1 M NaOH and 75 g of ice. The resulting mixture was stirred for 1 h and the products were extracted with CH_2Cl_2 (3×50 mL). The combined organic extracts were washed with brine, dried over $MgSO_4$, and concentrated. The crude product was purified via recrystallization from CH_2Cl_2/hexanes to give 0.65 g (75%) of **1** as a yellow crystalline solid, mp 261–262 °C (lit.[14] mp: 260–261 °C): ^{1}H NMR (500 MHz, CD_2Cl_2) δ 8.42 (d, 2H, J = 9.2 Hz), 6.81 (d × d, 2H, J = 2.4, 9.2 Hz), 6.74 (d, 2H, J = 2.4 Hz), 3.11 (s, 12H), ^{13}C NMR (125 MHz, CD_2Cl_2) δ 177.2, 151.7, 138.6, 130.3, 118.5, 110.9, 104.8, 39.6; IR (KBr) 1589 cm^{-1}; λ_{max} (EtOH) 377 nm.

4.1.14. Preparation of bis-2,7-dimethylaminoselenoxanthen-9-one (2). Phosphorus oxychloride (2.4 mL, 26 mmol) and benzamide **14** (1.09 g, 2.6 mmol) were heated at reflux in 30 mL of acetonitrile for 1.5 h. Workup as described above gave 0.66 g (73%) of **2**, mp 224–225 °C (lit.[16] mp: 224–225 °C): ^{1}H NMR (500 MHz, CD_2Cl_2) δ 8.38 (d, 2H, J = 8.9 Hz), 6.80 (d × d, 2H, J = 8.9, 1.2 Hz), 6.75 (d, 2H, J = 1.2 Hz), 3.11 (s, 12H); ^{13}C NMR (CD_2Cl_2) δ 179.1, 151.6, 136.1, 131.6, 119.9, 111.0, 107.5, 39.5; IR (KBr) 1592 cm^{-1}; λ_{max} (EtOH) 388 nm.

4.2. Quantum yield determination for the generation of singlet oxygen

The quantum yields for the generation of singlet oxygen for **TMR-S**, **TMR-Se**, and **3**–**12** were measured by direct methods in methanol or chloroform.[19] A SPEX 270M spectrometer (Jobin Yvon) equipped with InGaAs photodetector (Electro-Optical Systems, Inc., USA) was used for recording singlet oxygen emission spectra. A diode-pumped solid-state laser (Millenia X, Spectra Physics) at 532 nm was the excitation source. The sample solution in a quartz cuvette was placed directly in front of the entrance slit of the spectrometer and the emission signal was collected at 90° relative to the exciting laser beam. An additional longpass filter (850LP) was used to attenuate the excitation laser and the fluorescence from the photosensitizer.

4.3. Fluorescence quantum yields

Fluorescence quantum yields (ϕ_F) were measured using techniques and equipment that we have previously described.[20]

4.4. Cells and culture conditions

Cultured cells used in this study were the Chinese hamster ovary parental cell line AUXB1,[21] a chemosensitive cell line that has a very low Pgp content and the multidrug-resistant subline, CR1R12, which highly constituitively expresses Pgp. Multidrug-resistant CR1R12 cells were established from the CH^{R}C5 cell line[22] by sequential culturing in increasing concentrations of colchicine with 5μg mL^{-1} being the final concentration used. Cell lines were maintained in passage culture on 60 mm diameter polystyrene dishes (Corning Costar, Corning, NY, USA) in 3.0 mL minimum essential medium (α-MEM) supplemented with 10% fetal bovine serum (FBS), 50 units mL^{-1} penicillin G, 50 μg mL^{-1} streptomycin and 1.0μg mL^{-1} Fungizone® (complete medium). Only cells from passages 1–10 were used for experiments. A stock of cells, passages 1–4, were maintained at −86 °C to initiate experimental cultures. Cultures were maintained at 37 °C in a 5% CO_2 humidified atmosphere (Forma Scientific, Marietta, OH, USA). Passage was accomplished by removing the culture medium, then adding a 1.0 mL solution containing 0.25% trypsin, incubating at 37 °C for 2–5 min to remove cells from the surface, and seeding new culture dishes with an appropriate number of cells in 3.0 mL of complete medium. Cell counts were performed using either a hemocytometer or a particle counter (Model ZM, Coulter Electronics, Hialeah, FL, USA).

4.5. Determination of intracellular dye content

Cell lines, AUXB1 and CR1R12, were seeded on 96-well plates in 200 μL per well complete medium at $1–4 \times 10^4$ cells per well. Twenty-four hours after seeding, verapamil at 50 μM was added to selected wells in complete medium and cultures were incubated in the dark at 37 °C for 15 min. Dyes were then added to the cultures at various concentrations in complete medium. Cells were incubated in the dark at 37 °C for 2 h with or without verapamil in the presence of selected dyes. The medium was then removed and the monolayers washed once with 200 μL 0.9% NaCl and 200 μL 0.9% NaCl were added. The fluorescence of the intracellular dye was determined using a multiwell fluorescence plate reader (Gemini, Molecular Devices, Palo Alto, CA, USA). The excitation/emission wavelengths were set appropriately for each dye. Intracellular dye content was determined by comparing the magnitude of the fluorescence signal measured in each well to the fluorescence signal emitted from known concentrations of dye and calculating the femtomoles of intracellular dye per cell from those values.

4.6. Photoradiation of cell cultures

Cell lines, AUXB1 and CR1R12, were seeded on 96-well plates in 200 μL per well complete medium at $1–4 \times 10^4$ cells per well. Following treatment with or without 1×10^{-5} M verapamil, **TMR** analogues were then added directly to the cell culture medium at various concentrations and incubated for 2 h in the dark as above. The medium was then removed and 200 μL α-MEM minus FBS and phenol red (clear medium) were added to each well. One plate, with the lid removed, was then exposed to 350–750 nm light delivered at 1.4 mW cm^{-2} for 1 h (5.0 J cm^{-2}) from a filtered tungsten/halogen source, while a parallel plate was kept in the dark during the

irradiation period. Immediately following irradiation, the clear medium was replaced with complete medium and the monolayers were incubated for an additional 24 h period. Subsequently, cells were trypsinized and the MTT assay was used to determine cell viability. Data are expressed as percent cell viability compared to control cells which had been exposed to neither dye nor light.

Acknowledgments

This research was supported by the Department of Defense [Breast Cancer Research Program] under award number (W81XWH-04-1-0708). Views and opinions of and endorsements by the author(s) do not reflect those of the US Army or the Department of Defense.

References and notes

1. Gottesman, M. M.; Fojo, T.; Bates, S. *Nat. Rev. Cancer* **2002**, *2*, 48.
2. Dong, J.; Yang, G.; Mchaourab, H. S. *Science* **2005**, *308*, 1023.
3. Reyes, C. L.; Chang, G. *Science* **2005**, *308*, 1028.
4. Burger, H.; Foekens, J. A.; Look, M. P.; Meijer-van Gelder, M. E.; Klijn, J. G. M.; Wiemer, E. A. C.; Stoter, G.; Nooter, K. *Clin. Cancer Res.* **2003**, *9*, 827.
5. Borges-Walmsley, M. I.; McKeegan, K. S.; Walmsley, A. R. *Biochem. J.* **2003**, *376*, 313.
6. Larsen, A. K.; Escargueil, A. E.; Skladanowski, A. *Pharm. Ther.* **2000**, *85*, 217.
7. Goldstein, L. J. *Eur. J. Cancer* **1996**, *32A*, 1039.
8. Leonard, G. D.; Fojo, T.; Bates, S. E. *Oncologist* **2003**, *8*, 411.
9. Ford, J. M. *Eur. J. Cancer* **1996**, *32A*, 991.
10. Loetchutinat, C.; Saengkhae, C.; Marbeuf-Gueye, C.; Garnier-Suillerot, A. *Eur. J. Biochem.* **2003**, *270*, 476.
11. Martin, C.; Walker, J.; Rothnie, A.; Callaghan, R. *Br. J. Cancer* **2003**, *89*, 1581.
12. Lu, P.; Liu, R.; Sharon, F. J. *Eur. J. Biochem.* **2001**, *268*, 1687.
13. Detty, M. R.; Gibson, S. L.; Hilf, R. *Bioorg. Med. Chem.* **2004**, *12*, 2580.
14. Detty, M. R.; Prasad, P. N.; Donnelly, D. J.; Ohulchanskyy, T.; Gibson, S. L.; Hilf, R. *Bioorg. Med. Chem.* **2004**, *12*, 2537.
15. Gibson, S. L.; Hilf, R.; Donnelly, D. J.; Detty, M. R. *Bioorg. Med. Chem.* **2004**, *12*, 4625.
16. Brennan, N. K.; Donnelly, D. J.; Detty, M. R. *J. Org. Chem.* **2003**, *68*, 3344.
17. Singlet oxygen lifetimes are too short in water to allow meaningful quantum yield determinations by direct methods in that solvent. Methanol is used to approximate the polarity and hydrogen bonding found in water. In 50% aq MeOH, $\phi(^1O_2)$ for **TMR-S** and **TMR-Se** was measured as 0.18 ± 0.05 and 0.83 ± 0.07, respectively, using indirect methods via diphenylisobenzofuran adducts with rose Bengal as a standard. These values are identical, within experimental error, to the values of $\phi(^1O_2)$ obtained by direct methods in MeOH suggesting that values of $\phi(^1O_2)$ obtained in MeOH, are a good approximation for values obtained in aqueous solvent. For indirect methods with diphenylisobenzofuran, see: Leonard, K. A.; Hall, J. P.; Nelen, M. I.; Davies, S. R.; Gollnick, S. O.; Oseroff, A. R.; Gibson, S. L.; Hilf, R.; Chen, L. B.; Detty, M. R. *J. Med. Chem.* **2000**, *43*, 4488.
18. Guggenheim, T. L. *Tetrahedron Lett.* **1984**, *25*, 1253.
19. Pandey, R. K.; Sumlin, A. B.; Constantine, S.; Aoudia, M.; Potter, W. R.; Bellnier, D. A.; Henderson, B. W.; Rodgers, M. A.; Smith, K. M.; Dougherty, T. J. *Photochem. Photobiol.* **1996**, *64*, 194.
20. Ohulchanskyy, T.; Donnelly, D. J.; Detty, M. R.; Prasad, P. N. *J. Phys. Chem. B* **2004**, *108*, 8668.
21. Essodaigui, M.; Broxterman, H. J.; Garnier-Suillerot, A. *Biochemistry* **1998**, *37*, 2243.
22. Homolya, L.; Hollo, Z.; Germann, U. A.; Pastan, I.; Gottesman, M. M.; Sarkadi, B. *J. Biol. Chem.* **1993**, *268*, 21493.